Histol Histopathol (2010) 25: 309-320
DOI: 10.14670/HH-25.309

http://www.hh.um.es

Histology and Histopathology
Cellular and Molecular Biology

Comparison of the tumorigenic potential of liver and kidney tumors induced by N-nitrosodimethylamine

Gyorgy Trencsenyi[1], Tamas Juhasz[2], Fruzsina Bako[1], Terez Marian[3], Istvan Pocsi[1], Pal Kertai[4], Janos Hunyadi[5] and Gaspar Banfalvi[1]

[1]Department of Microbial Biotechnology and Cell Biology, [2]Department of Anatomy, Histology and Embryology, [3]Institute of Nuclear Medicine, [4]Institute of Preventive Medicine and [5]Department of Dermatology, University of Debrecen, Debrecen, Hungary

Summary. The aim of the study was to determine the tumorigenic potential of two cell lines established from N-nitrosodimethylamine induced rat hepatocarcinoma (HeDe) and mesenchymal renal tumors (NeDe). The basis of the distinction is that human cancers are known to overexpress facilitative GLUT transporters and TGF-ß1 protein. These proteins are linked to the increased metabolic energy consumption indicating uncontrolled growth and proliferation. We have assayed not only the expression of GLUT-1, GLUT-3 and TGF-ß1 proteins, but also the uptake of 2-fluoro-[^{18}F]-2-deoxi-D-glucose (^{18}FDG), a tracer for cancer diagnosis. Western blot analysis and whole body autoradiography were used to measure the ^{18}FDG uptake of tumor cells. Elevated ^{18}FDG uptake was measured in both tumor cell lines. Whole body autoradiography provided evidence that the uptake of ^{18}FDG was lower in the necrotic inner part than in the more vascularized outer parts of primary hepatocarcinoma and mesenchymal renal tumors. GLUT-1 overexpression in hepatocarcinoma tumor, and high levels of GLUT-3 were found in the NeDe cell line and in the mesenchymal renal tumor. TGF-ß-1 was overexpressed in hepatocarcinoma and mesenchymal renal tumors. *In vitro* and *in vivo* parameters support the view that the tumorigenic potential of cancer cells cannot be determined by the expression of a single parameter such as the expression of either GLUT-1, GLUT-3 or ^{18}FDG uptake. Besides the tumorigenic potential of the hepatocarcinoma, the high metabolic activity of the renal tumor indicated by its ^{18}FDG uptake, GLUT-3 and TGF-ß1 expression, the mesenchymal renal tumor induced by N-nitroso-dimethylamine is not a benign, but an an aggressive renal carcinoma.

Key words: Chemical induction, Primary tumor, Tumor cell lines, Gene expression, GLUT transporters, ^{18}FDG uptake, Whole body autoradiography

Offprint requests to: Prof. Gaspar Banfalvi PhD, DSc, Deprtment of Microbial Biotechnology and Cell Biology, University of Debrecen, 1 Egyetem Square, Debrecen 4010 Hungary. e-mail: bgaspar@delfin.klte.hu

Introduction

N-nitrosodimethylamine is a transplacental carcinogen inducing lung, liver and kidney tumors when administered to rodents (Tomatis, 1973). N-dimethynitrosoamine is present in food, tobacco smoke, and in different environmental sources (Diaz Gomez et al., 1986). Its constant presence underlines the prognostic relevance for patients with liver, renal or lung carcinoma. The increased incidence of lung, liver, kidney and nasal cavity tumors induced by N-dimethynitrosoamine were observed in mice, rats, hamsters, rabbits, guinea pigs, newts, fish etc (Table 1). When rats at newborn age were administered intraperitoneally N-nitrosodimethylamine, hepato-carcinoma and mesenchymal mesoblastic renal carcinoma development was observed (Hard and Buttler, 1970, 1971a,b; Dezso et al., 1990; Paragh et al., 2003; Trencsenyi et al., 2007). However, it remained to be decided whether the liver or the kidney is the primary target of the carcinogenic effect caused by N-nitrosodimethylamine. We have observed that the primary tumor growth of hepatocarcinoma was slower than the faster growing mesenchymal renal tumor (Trencsenyi et al., 2009). Nevertheless, based on their growth rates we could not decide wether the liver or the kidney tumor cells induced with N-nitrosodimethyl-amine has a higher tumorigenic potential.

Although, the hepatocellular carcinoma is of global

concern, the majority of patients suffer in this unresectable disease due to the tumor stage or liver cirrhosis. Consequently, the prognosis of such patients is poor (Usatoff and Habib, 2000). Among the primary tumors of the kidney, epithelial, adult's mesenchymal and children's nephroblastoma (Wilm's tumor) occur more frequently. Mesenchymal mesoblastic nephroma primary tumors are considered benign tumors, although the neoplasm induced with N-dimethynitrosoamine was characterized as an aggressive, malignant embryonal sarcoma (Hard and Butler, 1970, 1971a,b; Hard, 1985; Dezso et al., 1990).

After the surgical implantation of either hepatocarcinoma (HeDe) or mesenchymal renal carcinoma (HeDe) cells under the kidney capsule rapid tumor growth was observed. The complex and adaptive microenvironment inside the tumors made the estimation of malignant tumor progression difficult. Spatial and temporal variations in nutrient and waste gradients influence tumor growth. Consequently, distinction between the agressiveness of the two tumor cell types based on *in vivo* or *in vitro* growth could not be made. To distinguish between the tumorigenic potential of the two tumors more reliable parameters have been measured, such as the metabolic energy and the expression of specific gene products.

One of the major reasons for using 2-fluoro-[^{18}F]-2-deoxy-D-glucose (^{18}FDG) in tumor diagnostic measurements, such as positron emission tomography (Conti et al., 1996), is that several tumor cell lines, due to their higher rate of carbohydrate metabolism, have been shown to take up significantly higher levels of this glucose analogue than normal cells. This measurement provides an easily detectable contrast between normal and malignant cells *in vivo*. Experimental studies have shown that ^{18}FDG is a good tracer for cancer diagnosis (Som et al., 1980; Larson et al., 1981; Fukuda et al., 1982; Gallowitsch et al., 2003). To estimate the tumorigenic potential, the ^{18}FDG uptake and expression of facilitative glucose transporters have been suggested (Rastogi et al., 2007). Among the twelve known GLUT transporters the GLUT-1 and GLUT-3 transporters are the predominant factors, taking up more ^{18}FDG than other GLUT transporters, suggesting that that ^{18}FDG uptake of cultured tumor cells is governed by GLUT expression, and is a distinct characteristic of the neoplastic process (Waki et al., 1998). Data from several lines of studies indicate that malignant cells that are known to take up an increased amount of ^{18}FDG have overexpressed GLUT-1 and/or GLUT-3 (Yamamoto et al., 1990; Nishioka et al., 1992; Brown and Wahl, 1993; Waki et al., 1998; Rastogi et al., 2007). Increased expression of GLUT-1 and GLUT-3 has been reported in many human cancers. Overexpression of GLUT-1and GLUT-3 is associated with poor survival.

The GLUT-1 glucose transporter is responsible for the basal uptake and storage of glucose in all mammalian cells, especially in erythrocytes and in the hemochorial placenta (von Wolff et al., 2003; Mückler, 1990; Hahn and Desoye, 1996). The expression of GLUT-1 was highest in tumors among other glucose transporters (Rastogi et al., 2007). Moreover, it was found that ^{18}FDG uptake and the extent of GLUT-1 expression was proportional to the rate of tumor growth (Clavo et al., 1995).

GLUT-3 is a high affinity glucose transporter present in elevated levels in tissues which have a relatively high rate of glucose metabolism, such as brain, testes and placenta (Maher et al., 1992; Burant and Davidson, 1994; Boileau et al., 1995; Hauguel-de Mouzon et al., 1997; von Wolff et al., 2003). Elevated GLUT-3 levels were registered in breast tumor (Wahl, 1996; Meneses et

Table 1. The carcinogenic effect of N-nitrosodimethylamine in different animals.

Administration	Tumor	Animals
intramuscular	hemangiomas in liver, abdominal tissue, lung tumor	adult mice
	parenchymal tumors of liver, lung adenomas	newborn and suckling mice
	kidney tumors	adult rats
	kidney and liver tumors	newborn and suckling rats
	hemangiosarcoma in liver, bile duct and nasal tumor	hamster
	bile duct tumor	mastomys
intraperitoneal	liver tumor	adult and newborn mice
	lung and kidney tumors	mice
	liver tumor	newts
	kidney and nasal cavity	rats
oral	kidney and bile duct tumors	rats, hamsters
	hepatocellular carcinoma, bile duct tumor	rabbits, guinea pigs
	hemangiosarcoma	ducks
	liver adenoma, adenocarcinoma	fish
inhalation	lung, liver, kidney, nasal cavity	rats

These data come from animal experiments. No adequate human studies have been reported. N-nitrosodimethylamine is reasonably anticipated to be a human carcinogen (IARC, 1978, 1982; Peto et al., 1984; Sittig, 1985).

al., 2008), in ovarian carcinoma (Tsukioka et al., 2007) and in bronchioloalveolar lung cancer (Khandani et al., 2007). GLUT-3 has a limited expression not only in normal cells but also in malignant human tissues. It seems to play a role in glucose uptake in a subset of carcinomas of the lung, stomach and ovary with distinct clinical behavior (Younes et al., 1997).

There is evidence that TGF-ß1 plays a role as a tumor suppressor in early disease and has pro-oncogenic effects in advanced tumor stage. In the context of hepatocarcinogenesis, growth factors normally present at low or undetectable levels in normal human liver tissue become highly expressed in hepatoma cell lines, chemical models of hepatocarcinogenesis, and in human hepatocellular carcinoma (Rizzino, 1993). Patients with metastatic disease showed elevated TGF-ß1 protein expression in different tumor tissues (Langenskiöld et al., 2008), indicating that TGF-ß1 expression could be used as a potential metastatic tumor indicator.

Based on the relationship between the increased uptake of ^{18}FDG, elevated GLUT and TGF-ß1 expression in tumor cells, our objective was to use these parameters: a) to confirm or to disprove that a similar correlation exists in hepatocarcinoma (HeDe) and mesenchymal renal tumor cells (NeDe), b) to determine which of the two tumor cells (HeDe or NeDe) has a higher tumorigenic potential. The paper describes the characterization of two rat tumor cell lines differing in the expression of GLUT-1 and GLUT-3. The cancer cells were implanted in rat renal capsules and the uptake of ^{18}F-FDG was studied in tumors generated. The uptake of ^{18}FDG in tumors has been shown to be significantly lower in the necrotic inner part than in the more vascularized outer part of primary hepatocarcinoma and mesenchymal renal tumors.

Materials and methods

Chemicals and reagents

Reagents and inorganic chemicals, N-nitroso-dimethylamine, collagenase type I, hyaluronidase type IV, DNase type I, penicillin and streptomycin were purchased from Sigma-Aldrich Co. (St. Louis, MO). The growth media utilized gentamicin and fetal calf serum and were obtained from GIBCO BRL, Life Technologies (Gaithersburg, MD). Collagenase Medium consisted of RPMI 1640 medium containing 0.1% collagenase type I, 0.01% hyaluronidase type IV, 0.01% DNase I, 100 U/ml penicillin and 100 μg/ml streptomycin. For immunocytochemistry, immunohistochemistry and Western-blot analysis the following reagents were used. Monoclonal antibody to GADPH-loading control were obtained from Sigma-Aldrich Zrt. (Budapest, Hungary). Bovine serum albumin (BSA) was the product of Fermentas International Inc. (Burlington, Canada). Polyclonal rabbit anti-rat-GLUT-1, anti-rat-GLUT-3 and anti-TGF ß1 were bought from Abcam Inc. (Cambridge, MA, USA). Texas red-conjugated anti-rabbit secondary antibody and Vectashield Hard Set mounting medium containing DAPI were from Vector Laboratories, Ltd. (Peterborough, England), anti-rabbit IgG from Bio-Rad Laboratories (Hercules, CA, USA), and enhanced chemiluminescence reagent was purchased from Pierce, (Rockford, IL., USA). The positron emitting glucose analog 2-[^{18}F]fluoro-2-deoxy-D-glucose (^{18}FDG) was synthesized and labeled with the positron decaying isotope ^{18}F according to Hamacher et al. (1986).

Phosphate buffered saline (PBS) contained: 140 mM NaCl, 5 mM KCl, 8 mM Na_2HPO_4 and 3 mM NaH_2PO_4 at pH 7.3. Phosphate buffered saline with Tween (PBST) consisted of 0.1 % Tween 20, 20 mM Na_2HPO_4, 115 mM NaCl; pH 7.4. Five-fold concentrated electrophoresis buffer for Western blot analysis contained 20 mM Tris-HCl pH 7.4, 0.01 % bromophenol blue dissolved in 10% SDS, 100 mM ß-mercapto-ethanol. Components of blocking agent were: 5% non-fat dry milk in PBST (PBS, 0.1% Tween 20, 20 mM Na_2HPO_4, 115 mM NaCl; pH 7.4). The Collagenase Solution for perfusion contained 30mg collagenase type IV in 100 ml PBS solution.

Western blot analysis

Total cell lysates were subjected to Western blot analysis. Samples for SDS-PAGE were prepared by the addition of 100 μl five-fold concentrated electrophoresis buffer to cell lysates and boiled for 10 min. About 60 μg of protein was loaded onto 7.5% SDS-PAGE gel for the detection of GLUT-1 and GLUT-3. Proteins were transferred electrophoretically to nitrocellulose membranes. After non-specific blocking in 5% non-fat dry milk in PBST, membranes were washed and exposed to primary antibodies overnight at 4°C. Polyclonal anti-GLUT-1 antibody at a 1:250 dilution, polyclonal anti-GLUT-3 at a 1:400 dilution were used. After washing for 30 min with PBST, the membranes were incubated with anti-rabbit IgG for 1 h at room temperature in a 1:1000 dilution of PBS containing 1% non-fat dry milk. Signals were detected using an enhanced chemiluminescence reagent according to the instructions of the manufacturer. Freshly isolated fibroblast cells served as a negative control.

Glyceraldehyde 3-phosphate dehydrogenase (GAPDH) was used as positive control. Housekeeping proteins like GAPDH are useful as loading controls for Western blots and protein normalization. 50 μl monoclonal antibody to GADPH solution containing 50% glycerol, 0.01% thimerosal and 1.0 mg/ml BSA was applied for Western blot at 1:1000 dilution.

Induction of hepatocellular and mesenchymal renal tumor formation

N-nitrosodimethylamine is found in one of the more than a thousand National Priorities List sites identified by the Environmental Protection Agency. It causes liver, kidney, and occasionally lung cancers (Magee and

Barnes, 1962; Diaz Gomez et al., 1986). Toxicity data of N-nitrosodimethylamine can be found at the Agency for Toxic Substances and Disease Registry (www.atsdr.cdc.gov/toxfaq.html).

Establishment of HeDe and NeDe cell lines

Freshly resected hepatocarcinoma (HeDe) and mesenchymal renal carcinoma (NeDe) tissue was minced into small (2x2 mm) pieces and digested for 3 h at 37°C in collagenase medium. The mixture was filtered through four layers of sterile gauze, washed, and resuspended in RPMI 1640 medium supplemented with 10% FBS and antibiotics. After overnight incubation at 37°C in a 5% carbon dioxide (CO_2) atmosphere, the nonadherent cells were discarded and the adherent cells were subcultured. After 50 subcultures the new cell lines HeDe and NeDe were established. Cells isolated from hepatocellular and mesenchymal renal tumors will be heretofore referred to as HeDe and NeDe tumor cells to distinguish them from HeDe and NeDe cell lines.

Experimental surgery

For transplantation 10^6 cells (HeDe or NeDe cell line) in 10 μl were placed on the Gelaspon® disc. Experimental animals were anesthesized by intraperitoneal administration of pentobarbital (Nembutal) 3 mg/100g body weight. The abdomen was opened, the kidney was pulled out, the tumor cell containing gelatin disc was placed under the renal capsule and the kidney was placed back in the abdominal cavity (Slagel et al., 1985; Uzvolgyi et al., 1990). Stitches were put in the wound and autopsy was carried out two weeks later.

Isolation of F344 rat fibroblast cells

As control, freshly isolated rat fibroblast cells were used. A pregnant rat (7 days of pregnacy) was anesthetized, embryos were removed and placed in sterile PBS. Embryos were minced into small (2x2 mm) pieces and digested for 3 h at 37°C in Hank's solution containing 0.25% trypsin. The cell suspension was filtered through four layers of sterile gauze, washed, resuspended in RPMI 1640 medium supplemented with 10% FBS and antibiotics. After overnight incubation at 37°C in a 5% carbon dioxide atmosphere, the nonadherent cells were discarded and adherent cells were used as control.

Flow cytometry

A modified Becton Dickinson FACStar plus flow cytometer (Becton Dickinson, Mountain View, California) equipped with an argon ion laser was used to perform flow cytometric analysis and to determine fluorescence intensities. Emission was detected through a 620 nm long pass filter for propidium iodide.

Cell cycle analysis

Cells were fixed in 70% cold ethanol and kept at -20°C until use. Before the flow cytometry run, pelleted cells (10^6 cells) were suspended in PBS and treated with 100 μg/ml RNase for 30 min at 37°C and stained with 50 μg/ml propidium iodide (Marian et al., 2000). Flow cytometric data were analyzed using WinMDI version 2.8. and FCA version 2.2 (University of Debrecen, PET Center). Cell cycle analysis of DNA histograms was performed using the Cylchred version 1.0.2. programm (Automatic Cell Cycle Analysis software, Cardiff University).

In vitro uptake of ^{18}FDG glucose analogue

Exponentially growing, daily subcultured HeDe and NeDe cells were used for the *in vitro* uptake of glucose analogue. Cells of the hepatocellular HeDe cell line and the mesenchymal NeDe cell line were washed and resuspended in PBS. Freshly isolated fibroblasts served as control. Samples (10^6 cells in 1ml) were preincubated at 36°C for 10 minutes in PBS containing 1 mM α-D-glucose. Preincubation was followed by the addition of 185 kBq ^{18}FDG to each sample. After the addition of the radiotracer, the cells were incubated at 36°C for 15, 30 and 60 minutes and the uptake was terminated by the addition of 10 ml ice-cold PBS. Cells were washed three times with cold PBS, resuspended in 1 ml cold PBS and the radioactivity was measured. In a separate experiment the uptake of ^{18}FDG was measured in the presence of 5 μM cytochalasin B, and the cells incubated for 60 min. The uptake of ^{18}FDG was expressed as percentage of the total radioactivity of ^{18}FDG added to the cells.

Immunocytochemistry

Hepatocarcinoma and mesenchymal nephroma cells were cultured on the surface of 20x20 mm rectangular coverglasses (Spectrum 3D, Debrecen). Cells were fixed in 4% paraformaldehyde for 15 min, then washed in PBS. Non-specific binding sites were blocked with PBS containing 1% bovine serum albumin at 37°C for 30 min. After washing with PBS cells were incubated with anti-GLUT-1 and anti-GLUT-3 antibodies at 4°C overnight. A 250-fold dilution of primary antibodies was applied. To visualize the primary antibodies Texas red conjugated secondary antibody was used at 1:1000 dilution.

Fluorescence microscopy

Cells were mounted in Vectashield Hard Set mounting medium containing DAPI to visualize the nuclei of cells. Images were visualized by fluorescence microscopy (Nikon Eclipse E800Nikon Corporation, Tokyo). All images were acquired using constant camera settings to allow for comparative analysis of staining intensities.

Distribution of ^{18}FDG in tissues

The *in vivo* distribution of ^{18}FDG was studied in F344 rats. Three rats were anesthetized and their lumbar areas were shaven prior to surgery. A Gelaspon disc containing HeDe cells (10^6) was placed under the left renal capsule of the first rat. Similarly, 10^6 NeDe cells were implanted under the left renal capsule of the second rat. In the third control rat a Gelaspon disc without tumor cells was placed under the left renal capsule. On day 7 after implantation, rats were anesthetized and radioligand (14.8 mBq of ^{18}FDG in 1 ml saline) was injected into the left femoral vein of each rat. Animals were euthanized 60 min after ^{18}FDG administration with 300 mg/kg intravenal injection of pentobarbital. Animals were dissected and various organs/tissues were removed. Plasma was obtained from blood by centrifugation (3000g, 2 min). The radioactivity of triplicate tissue samples (1 g) was measured by an energy selective gamma counter. Muscle samples were taken from the hind leg and tumor samples from hepatocellular and from mesenchymal renal tumors. The tissue uptake was expressed as a differential absorption ratio (DAR). DAR was calculated as:

$$DAR = \frac{\text{(accumulated radioactivity/g tissue)}}{\text{(total injected radioactivity/body weight)}}$$

Whole-body autoradiography

For whole-body autoradiography the implantation of tumor cells was carried out as described above. One week after the surgery F344 rats were administered intravenously (left femoral vein) with 14.8 MBq ^{18}FDG and 1 h after injection the animals were euthanized. Each animal was embedded in an ice-cold 1% carboxymethyl-cellulose solution. Frozen in liquid nitrogen, 60 μm thin cryostate sections (Leica CM 3600 cryomacrotome, Nussloch, Germany) were cut in the sagittal plane. Sections were exposed to phosphorimaging plates (GE Healthcare, Piscataway, NJ, USA). For anatomic correspondence true color images of the sections were also obtained by a transparency scanner (Epson Perfection 1640, EPSON Deutschland GmbH, Meerbusch, Germany). Autoradiography and transmission images were overlaid to fuse the functional and anatomical information. For phosphorimage analysis of selected sections the ImageQuant™ 5.0 (GE Healthcare, Piscataway, NJ, USA) image analyzing software was used.

Statistical analysis

Statistical analysis was performed using a 2-way ANOVA and Student's t test. Results were expressed as mean ± standard deviation (SD) (n=3) and a value of $p<0.01$ was considered significant.

Results

Distribution of cells in cell cycle stages

The stage of proliferation of HeDe, NeDe and fibroblast cells was determined by flow cytometry. As the glucose analogue (^{18}FDG) uptake is different at various stages of the cell cycle, it was necessary for each of these lineages to be in the same phase of the cell cycle, not only for the ^{18}FDG uptake, but also for the immunocytometric experiments.

Table 2 shows that in early exponentially growing cultures of HeDe, NeDe and fibroblasts, most of the cells were in S phase (~ 60-64%), 20-22% in the G1 phase and 16-19% in the G2 phase. The cell cycle

Table 2. Distribution of cell cycle phases in HeDe, NeDe and fibroblast cell cultures.

Cell cycle phase	HeDe (%)	NeDe (%)	Fibroblast (%)
G1	21.2±3	22.3±2	20.1±2
S	60.3±2	59.8±1	63.7±2
G2	18.5±1	17.9±1	16.2±1

The relative DNA content was expressed as percentages of cells in G1, S and G2 phases. The DNA content was measured by flow cytometry using propidium iodide staining described in the Materials and Methods. Data are presented as means ± SD of three independent experiments.

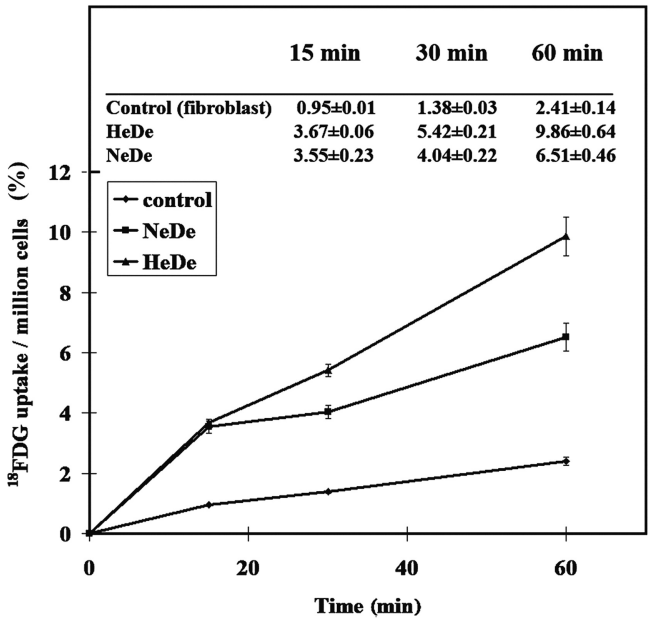

Fig. 1. The kinetics of ^{18}FDG uptake by fibroblasts, HeDe and NeDe cells. The uptake by 10^6 cells was expressed as the percentage of the total radiotracer added to the incubation mixture. Details of the experiment are given in the Methods. Data are presented as the means ± SD of three independent experiments. Differences were significant ($p<0.01$) at each time point of analysis between the control fibroblast and tumor cells.

distribution of the three cell types was similar, indicating that the proliferative activities of the three cell lines were comparable.

In vitro uptake of radiotracer glucose analogue

Exponentially growing, daily subcultured cells (Table 2) were used for the in vitro uptake of glucose analogue. Figure 1 shows that the incorporation of ^{18}FDG is approximately 4-times higher in hepatocarcinoma cells, and nearly 3-times higher in mesenchymal renal tumor cells than in control fibroblast cells. ^{18}FDG uptake indicates an aggressive growth rate and fast metabolism of HeDe and NeDe cell lines. The correlation of these data with the Western blot analysis will be shown below.

Cytochalasin B is a known inhibitor of glucose uptake in cells. Cytochalasin B was applied at a concentration of 5 μM to demonstrate that ^{18}FDG uptake can be suppressed not only in the primary fibroblast cells serving as a control, but also in HeDe and NeDe tumor cells. The ^{18}FDG uptake in these cells in the presence and in the absence of cytochalasin B is summarized in Table 3. As expected, this experiment proved that cytochalasin B inhibits glucose uptake in all three cell types. The ^{18}FDG incorporation was 7-11-times less in the presence than in the absence of this fungal metabolite.

Immunocytochemistry

Glucose uptake of cells takes place through specific GLUT transporters. Hepatocellular and mesenchymal kidney tumors have not been previously tested for

Table 3. ^{18}FDG uptake in the presence and absence of Cytochalasin B.

Cells	percentage/10^6 cells
Fibroblast	2.01±0.16
Fibroblast + 5μM Cytochalasin B	0.17±0.01
HeDe	6.96±0.34
HeDe + 5μM Cytochalasin B	0.66±0.05
NeDe	5.96±0.30
NeDe + 5μM Cytochalasin B	0.51±0.05

Data are presented as means ± S.D. (n=3). ^{18}FDG uptake of cells (10^6) was measured after 60 min incubation and expressed as the percentage of total radioactivity. Significant ($p<0.01$) differences were measured between the uptake of cytochalasin B treated and untreated fibroblast cells ($p=0.002$), between cytochalasin B treated and untreated HeDe cell line, and between cytochalasin B treated and untreated NeDe cell line ($p=0.001$ each).

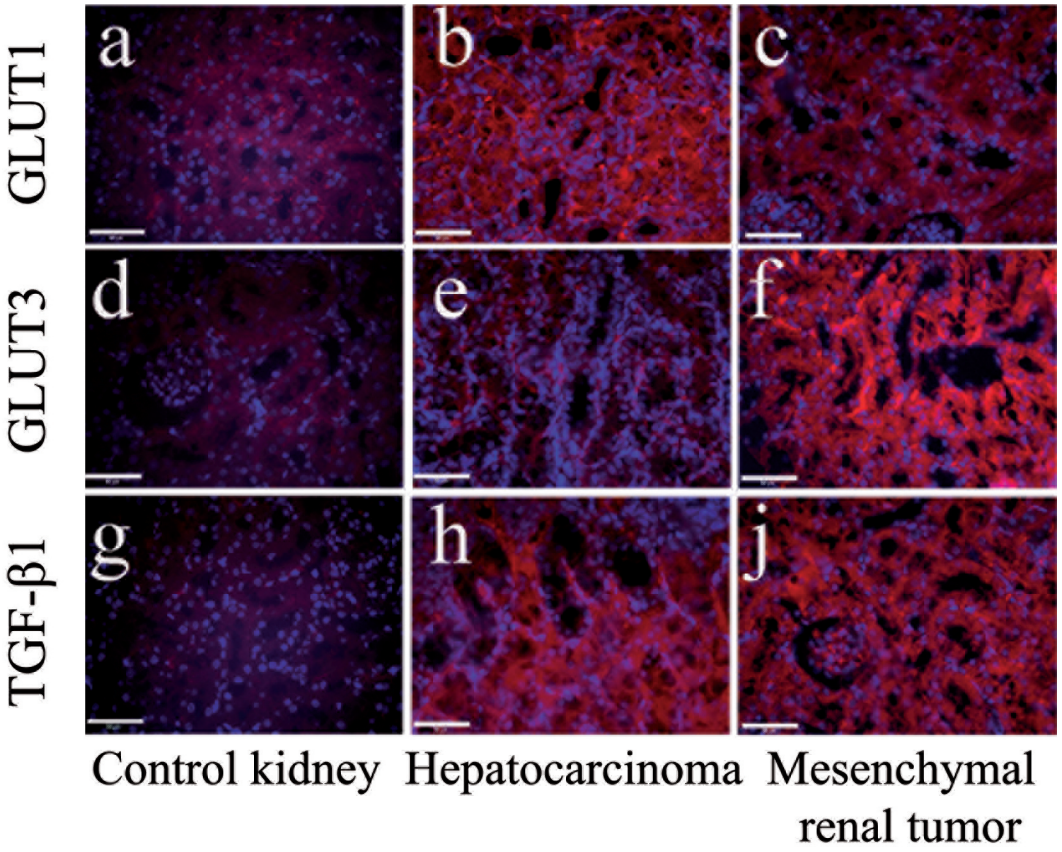

Fig. 2. Expression of GLUT-1, GLUT-3 and TGF-ß1 proteins in kidney sections of tumor-free rats and in hepatocarcinoma and mesenchymal kidney tumor-bearing rats. Nuclei of cells were stained with DAPI. GLUT transporters and TGF-ß1 were stained with Texas red conjugated antibodies. Bars: 50 μm.

GLUT transporters. The visualization of GLUT-1, GLUT-3 transporters and TGF-,1 expression was facilitated by the use of antibodies against these proteins (Fig. 2). Results obtained with this double labeling procedure revealed low levels of GLUT-1, GLUT-3 in the tissue sections of kidneys obtained from tumor-free rats (Fig. 2a,d,g). In the hepatocarcinoma tumor GLUT-1 and TGF-ß1 expression was high (Fig. 2b,h) relative to the low GLUT-3 expression (Fig. 2e). In the mesenchymal kidney tumor the GLUT-3 and TGF-,1 levels were high (Fig. 2f,j, respectively) with moderate expression of GLUT-1 transporter (Fig. 2c). These results were also supported by ^{18}FDG uptake and by Western blot analysis.

Western blot analysis

The expression of GLUT-1 and GLUT-3 glucose transporters was tested by Western blot analysis. We examined the levels of GLUT-1 and GLUT-3 in cell lysates prepared from fibroblasts, from the hepatocarcinoma and mesenchymal renal tumors and from the two cancer cell lines (HeDe, NeDe) using Western blot analysis (Fig. 3). GLUT-1 is the most widely expressed isoform of mammalian glucose transporters that provides cells with their basic glucose requirement. The expression of GLUT-1 was higher in the HeDe hepatocellular tumor than in the HeDe tumor cell line. GLUT-1 level was equally low in the NeDe cell line, in the mesenchymal kidney tumor and in fibroblast cells. The expression of GLUT-3 was low in fibroblast cells, hepatocarcinoma tumor in the HeDe cell line, significantly higher in the NeDe cell line and very high in mesenchymal renal tumor cells (Fig. 3).

GLUT-1 and GLUT-3 expression was hardly detectable in control fibroblast cells. Tumor cell lines expressed somewhat higher relative levels of GLUT transporters than the control cells. Significant differences were observed among the expressions of the tumors and the tumor cell lines. The hepatocellular tumor cells expressed much more GLUT-1 transporters than the mesenchymal kidney tumor cells or the tumor cell lines. The level of GLUT-3 transporter was low in hepatocarcinoma cells, higher in tumor cell lines and highest in mesenchymal kidney tumor cells. All cell lines and tissues were positive for GADPH protein (Fig. 3).

Tissue distribution of ^{18}FDG

The *in vivo* distribution of ^{18}FDG was studied in tissues isolated from tumor-bearing F344 rats. After the administration of the radioligand the animals were euthanized, dissected and the differential absorption ratio (DAR) was determined in blood plasma, in muscle, in the living (outer) and in the necrotic (inner) parts of the HeDe and NeDe tumors. The biodistribution of ^{18}FDG in tumor-bearing rats was lowest in the resting muscle, followed by two times higher, but still low level in blood plasma (Fig. 4). In contrast, the high levels of ^{18}FDG in the living part of hepatocarcinoma (HeDe) and in the mesenchymal renal (NeDe) tumors reflected high *in vivo* proliferative activities. The inner and outer parts of the tumors could be anatomically well distintinguished and separated and their metabolic potential could be tested by measuring the DAR values. The inner part of the tumors was necrotic after one week of tumor cell implantation. The outer living part of the hepatocellular

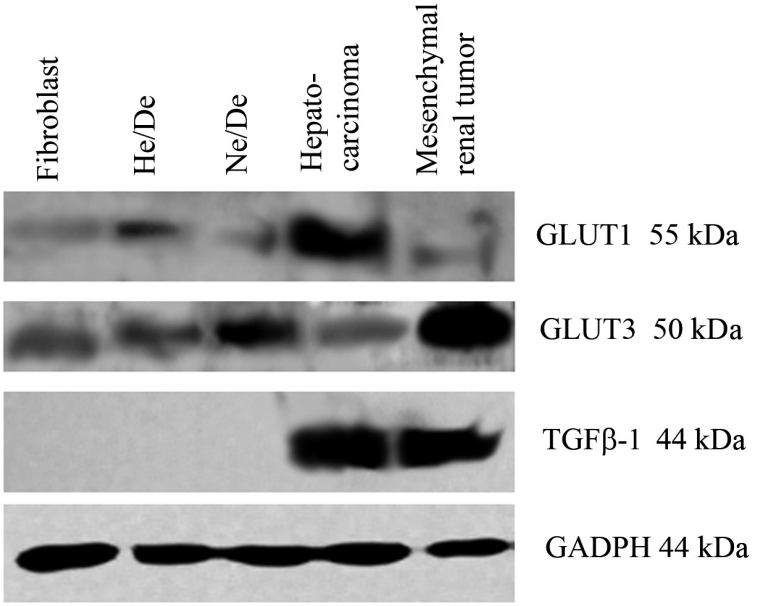

Fig. 3. Western blot analysis of GLUT-1, GLUT-3 and TGF-ß1 in fibroblast, HeDe and NeDe cell lines and in hepatocellular and mesenchymal renal tumors. Cell homogenates were prepared as described in the Methods. Western blot analysis was performed using anti-GLUT-1, anti-GLUT-3 and anti-TGF-ß1 antibodies. GADPH antibody was used as a protein loading control, as it does not change significantly. Total proteins from various rat tissue lysates and cells were normalized using the GADPH monoclonal antibody.

tumor accumulated 25-28-times more ^{18}FDG than the inner necrotic part. The living part of the mesenchymal renal tumor was also at least 15-times more active metabolically than its necrotic inner part (Fig. 4).

Whole-body autoradiography

Rats were treated the same way as described above for the tissue distribution studies with the exception that tumor-bearing euthanized animals were not dissected. Bodies of rats were embedded in carboxymethyl-cellulose solution, frozen in liquid nitrogen and cut in the sagittal plane. The radiotracer uptake was followed by whole body autoradiography. Sections were exposed to phosphorimaging plates, and for anatomic correspondence true color images of the sections were obtained by transparency scanning. Autoradiographic and transmission images were overlaid to provide a combined view of the functional and anatomical distribution. The phosphorimage analysis of selected sections is shown in Fig. 5. The ^{18}FDG distribution in tumor-bearing rats showed high local concentration in the the kidney indicating its rapid clearance. The rapid metabolic rates of HeDe (Fig. 5a) and NeDe (Fig. 5e) tumors are clearly visible in the primary tumors developed under the kidney. The same autoradiographic pictures have been magnified for closer scrutiny in Fig. 5b and 5f. In Fig. 5b the hepatocellular tumor was seen first as a separate round body under the kidney, which later intruded into the kidney (KN). It is to be noted that the high ^{18}FDG concentration inside the kidney was found in the renal pelvis where the radiotracer is excreted and accumulates before being removed via the urine. Moreover, one can distinguish two parts of intrusion, the living cortical part (LP) and the inner necrotic part (NP). As far as the invasion and progression of the mesenchymal kidney tumor (NeDe) is concerned, it appears to be attached immediately to the kidney tissue and is less distinctive than the hepatocellular tumor (Fig. 5f).

Anatomical images serve to provide a view of selected regions of interest (ROI) (Fig. 5c,g). The program gives the results in pixels of the selected ROIs, and the average pixel density of the selected area. The number of pixels corresponds to the radioactivity of the selected regions of interest. As a unit of pixel density (radioactive counts/pixel) the resting muscle of the hind leg of the euthanized, tumor-bearing rat was chosen. The pixel density was high in tumors and in kidneys, but low in the resting muscle. The biodistribution of the radiotracer in HeDe whole tumor (WT) was 18-times higher than in the resting muscle taken as a unit. The pixel density shows that the uptake of the radiotracer in the living part (LP) of the HeDe tumor was 23-times and in the necrotic part (NP) 4-times higher than in the muscle (M). The glucose metabolism represented by the tracer uptake is almost 6-times higher in the outer living portion than in the inner necrotic region of the tumor (Fig. 5d). Similar results were obtained with NeDe tumor, where the whole tumor (WT) accumulated 14-times more ^{18}FDG than the muscle (Fig. 5h). The radiotracer uptake in the living part of the tumor was 17-times and in the necrotic part 2.8-times higher than in the muscle. The ratios between the living and necrotic parts were similar in the HeDe and NeDe tumors (Fig. 5d,h).

In control, tumor-free rats the radiotracer uptake was high in the kidney, similar to the tumor-bearing animals. The radiotracer in the control, tumor-free rats was evenly distributed in different tissues showing low levels (not presented). Measurements related to the biodistribution of ^{18}FDG in other tissues and organs of NeDe tumor-bearing rats are under investigation (Trencsenyi et al., unpublished results).

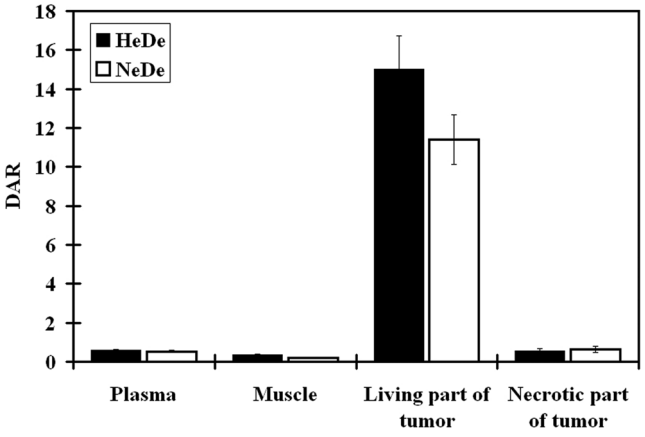

Fig. 4. Distribution of ^{18}FDG in blood plasma, muscle and in the tumors after HeDe or NeDe cell implantation. The radioactivity of triplicate tissue samples was measured in a gamma counter. The tissue uptake was expressed as differential absorption ratio (DAR) as described in the Methods.

Discussion

The tumorigenicity of two tumors (hepatocarcinoma, mesenchymal renal carcinoma) induced in rats by N-nitrosodimethylamine was originally judged by their growth at the primary site of tumor formation. Based on this criterion, when HeDe or NeDe cells were implanted under the kidney capsule of rats we have observed an immediate invasion of kidney by NeDe cells. HeDe cells implanted under the kidney capsule initiated first the growth of a separate hepatocellular tumor before invading the foreign kidney tissue. From the invasion of the kidney one would have expected NeDe cells to grow more agressively than HeDe cells. The implantation of tumor cells under the kidney capsule is a known and accepted method, but the tumorigenic potential of different tumors cannot be judged by this method. The measurements of Clavo et al. (1995) that the ^{18}FDG uptake and the extent of GLUT-1 expression were proportional to the level of tumor growth suggested a

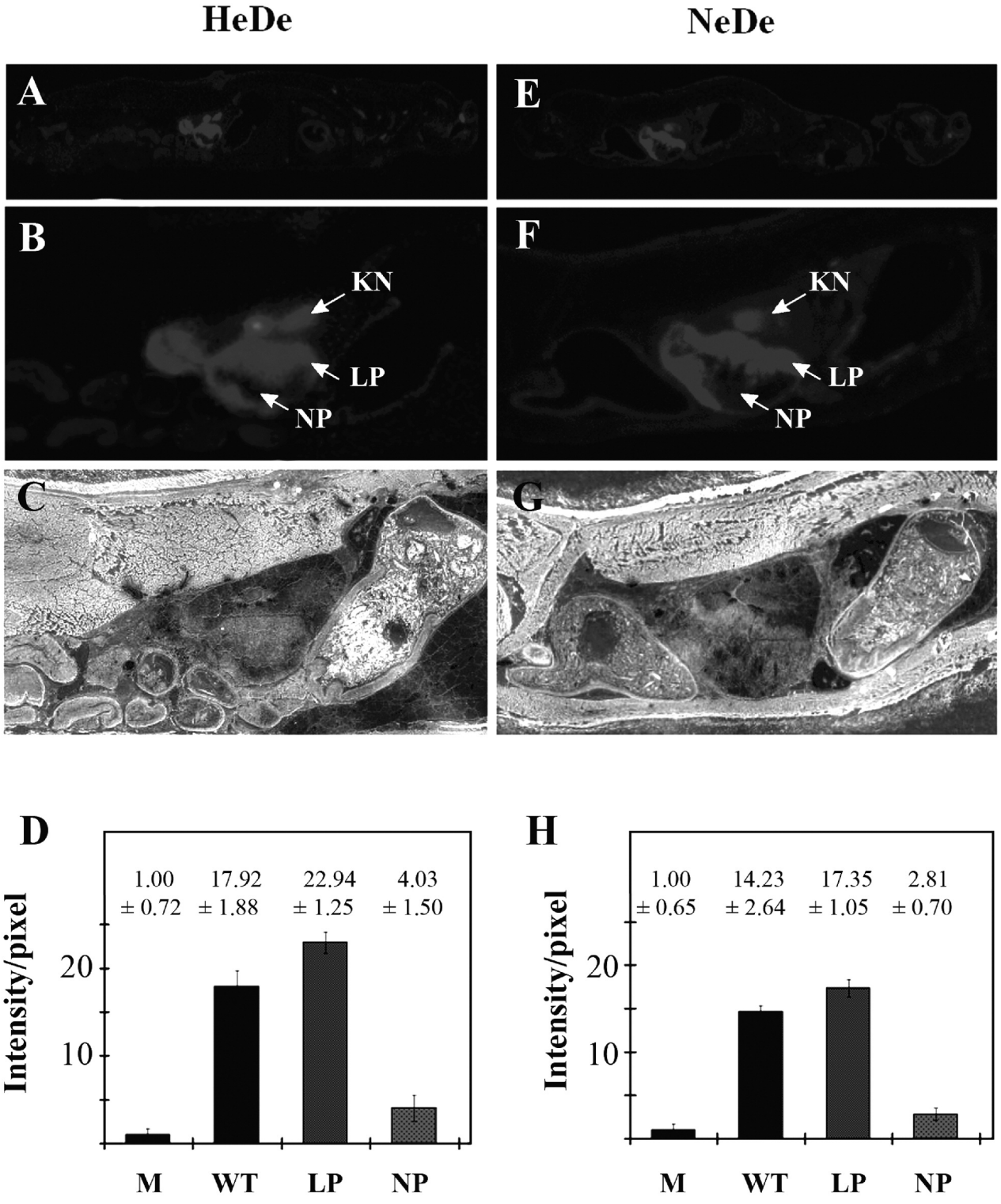

Fig. 5. Whole body autoradiogaphy showing the tissue distribution of ^{18}FDG in tumor-bearing rats. Tumor cells from HeDe and from NeDe cell lines were transplanted under the renal capsule of the left kidney, and after one week of tumor development 185 kBq ^{18}FDG was injected in the left femoral vein. One hour after the injection each animal was euthanized and whole body autroradiography was carried out as described in the Methods section. **a)** autoradiography of HeDe tumor-bearing rat, **b**) same as **a)** at higher magnification, **c)** true color image of the same section obtained with transparency scanner, **d)** phosphorimage analysis of tissues in HeDe tumor-bearing rat, **e)** autoradiography of NeDe tumor-bearing rat, **f**) same as e) at higher magnification, **g)** true color image of the same section obtained with transparency scanner, **h)** phosphorimage analysis of tissues in NeDe tumor-bearing rat. M, muscle; WT, whole tumor; LP, living part of tumor; NP, necrotic part of tumor.

reasonable approch to judge the tumorigenicity of HeDe and NeDe cells. Studies indicate that malignant cells with an increased uptake of 18FDG, have overexpressed GLUT-1 and/or GLUT-3 (Yamamoto et al., 1990; Nishioka et al., 1992; Brown and Wahl, 1993; Waki et al., 1998; Rastogi et al., 2007). Increased TGF-ß1 protein level in patients with colorectal cancer (Langenskiöld et al., 2008) also indicated that the overexpression of TGF-ß1 can be used as a diagnostic tool to estimate the tumor forming capability of certain tumors.

From the tumor growth we could not judge which of the two primary tumors (hepatocarcinoma, mesenchymal renal carcinoma) induced by N-nitrosodimethylamine has a higher tumorigenic potential. Thus we have chosen four tumor markers (^{18}FDG uptake, overexpression of GLUT-1, GLUT-3 and TGF-ß1) to estimate the agressiveness of the tumor forming capability of HeDe and NeDe tumor cell lines. The augmentation of GLUT-1 expression in hepatocarcinoma cells, elevated GLUT-3 levels in NeDe cells and in the mesenchymal kidney tumor were measured. Freshly isolated fibroblast cells served as negative control. As positive control for Western blot analysis and protein normalization the housekeeping protein GADPH was used. The high ^{18}FDG uptake in HeDe and NeDe tumors did not correlate with their GLUT-1 and GLUT-3 expression. In the hepatocarcinoma GLUT-1 expression was high, but GLUT-3 expression was low, while in mesenchymal renal carcinoma GLUT-3 expression was elevated and GLUT-1 level was low.

The elevated levels of GLUT-3 expression in those tissues and organs which have a relatively high rate of glucose metabolism, such as the kidneys (Maher et al., 1992; Burant and Davidson, 1994; Boileau et al., 1995; Hauguel-de Mouzon et al., 1997; von Wolff et al., 2003) could explain why GLUT-3 expression is even higher in the mesenchymal renal carcinoma. Kidneys not only sense the plasma concentration of glucose, but are actively involved in its metabolism and regulation.

^{18}FDG uptake was higher in both tumors relative to the control fibroblast cells. These data indicate that the expression of GLUT transporters *per se* is not sufficient to judge tumorigenicity. A more reliable relationship exists between tumorigenicity and TGF-ß1 expression. Similarly, the ^{18}FDG uptake portrays more realistically the malignant nature of tumor formation than the expression of individual GLUT transporters.

The uptake of ^{18}FDG indicates that hepatocellular (HeDe) tumor formation has a somewhat higher tumorigenic potential than the nephrotoxic tumor (NeDe). In both hepatocarcinoma and mesenchymal kidney tumors the growth rate was fast. Autoradiography revealed that there is a significant difference in the ^{18}FDG uptake in the inner necrotic and in the outer more vascularized part of HeDe and NeDe tumors. Our results contradict others, who have found that the central part of the tumor, which is thought to be relatively hypoxic, had stronger GLUT-1 expression and higher glucose uptake in the PET scan than the periphery, in both the primary tumor and in metastatic foci (Wahl, 1996; Rastogi et al., 2007). It was argued that the ^{18}FDG uptake is related to the size of the tumor and to GLUT-1 overexpression; as the tumor grows, its central part becomes less oxigenated, and hypoxia stimulates GLUT-1 overexpression and ^{18}FDG uptake (Gu et al., 2006). We have found higher ^{18}FDG uptake in the outer living part of HeDe and NeDe tumors than in the central necrotic part, indicating that tumor development depends primarily on the size, growth rate, vascularization and hypoxic conditions inside the tumor.

Conclusion

Our aim was to decide whether the mesenchymal kidney tumor induced by N-nitrosodimethylamine has a metastatic potential. To judge tumorigenicity, the growth rate of primary tumors is not a decisive factor, as tumor growth depends on several conditions. Thus, we have chosen the measurement of parameters which were thought to be typical to metastatic cells. From the oncogenic indicators, the elevated ^{18}FDG uptake, the increased expression of TGF-ß1 protein, GLUT-1 and GLUT-3 transporters have been selected. Our results show that GLUT-3 level was high in mesenchymal renal carcinoma, but was low in hepatocarcinoma. On the contrary, GLUT-1 was low in renal tumor but high in hepatocarcinoma. Tissue staining with Texas-red conjugated antibodies and Western blot analysis confirmed these observations.

Major conclusions are: a) Only elevated ^{18}FDG uptake and the increased expression of TGF-ß1 can be regarded as common tumorigenic indicators. b) The extremely high ^{18}FDG uptake in hepatocarcinoma was taken as evidence that the hepatocarcinoma induced by N-nitrosodimethylamine is the primary tumorigenic effect. c) The fact that ^{18}FDG uptake was also high in mesenchymal renal tumor indicates that the renal tumor induced by N-nitrosodimethylamine also has a metastatic potential and can be used as a renal metastatic tumor model. d) Finally, tumor growth is much faster in the outer living portion of these tumors than in the inner necrotic part, an indication that angiogenesis is directed toward the periphery of the tumor.

Acknowledgements. This work was supported by a grant of the Hungarian National Science and Research Foundation to G.B. (OTKA T42762 grant). The flow cytometric measurements by Dr. Zoltan Krasznai, the evaluation of cytometric data by Dr. Laszlo Balkay and the technical contribution of Tamas Nagy (PET Center) are gratefully acknowledged.

References

Agency for toxic substances and disease registry. www.atsdr.cdc.gov/toxfaq.html.

Boileau P., Mrejen C., Girard J. and Hauguel-De Mouzo S. (1995).

Overexpression of GLUT-3 placental glucose transporter in diabetic rats. J. Clin. Invest. 96, 309-317.

Brown R.S. and Wahl R.L. (1993). Overexpression of GLUT-1 glucose transporter in human breast cancer. An immunohistochemical study. Cancer 72, 2979-2985.

Burant C.F. and Davidson N.O. (1994). GLUT-3 glucose transporter isoform in rat testis: localization, effect of diabetes mellitus, and comparison to human testis. Am. J. Physiol. 267, 1488-1495.

Clavo A.C., Brown R.S. and Wahl R.L. (1995). Fluorodeoxyglucose uptake in human cancer cell lines is increased by hypoxia. J. Nucl. Med. 36, 1625-1632.

Conti P.S., Lilien D.L., Hawley K., Keppler J., Grafton S.T., and Bading, J.R. (1996). PET and [^{18}F]-FDG in oncology: a clinical update. Nucl. Med. Biol. 23, 717-735.

Dezso B., Rady P,. Morocz I., Varga E., Gomba S,. Poulsen K. and Kertai P. (1990). Morphological and immunohistochemical characteristics of dimethylnitrosamine-induced malignant mesenchymal renal tumor in F-344 rats. J. Cancer Res. Clin. Oncol. 116, 372-378.

Diaz Gomez M.I., Tamayo D. and Castro J.A. (1986). Administration of N-nitrosodimethylamine, N-nitrosopyrrolidine, or N'-nitroso-nornicotine to nursing rats: their interactions with liver and kidney nucleic acids from sucklings. J. Natl. Cancer Inst. 76, 1133-1136.

Fukuda H., Matsuzawa T., Abe Y., Endo S., Yamada K., Kubota K., Hatazawa J., Sato T., Ito M., Takahashi T., Iwata R. and Ido T. (1982). Experimental study for cancer diagnosis with positron-labeled fluorinated glucose analogs: [^{18}F]-2-fluoro-2-deoxy-D-mannose: a new tracer for cancer detection. Eur. J. Nucl. Med. 7, 294-297.

Gallowitsch H.J., Kresnik E., Gasser J., Kumnig G., Igerc I., Mikosch P. and Lind P. (2003). F-18 fluorodeoxyglucose positron-emission tomography in the diagnosis of tumor recurrence and metastases in the follow-up of patients with breast carcinoma: a comparison to conventional imaging. Invest. Radiol. 38, 250-256.

Gu J., Yamamoto H., Fukunaga H., Danno K., Takemasa I., Ikeda M., Tatsumi M., Sekimoto M., Hatazawa J., Nishimura T. and Monden M. (2006). Correlation of GLUT-1 overexpression, tumor size, and depth of invasion with 18F-2-fluoro-2-deoxy-D-glucose uptake by positron emission tomography in colorectal cancer. Dig. Dis. Sci. 51, 2198-2205.

Hamacher K., Coenen H.H. and Stocklin G. (1986). Efficient stereospecific synthesis of no-carrier-added 2-(^{18}F)-fluoro-2-deoxy-d-glucose using aminopolyether supported nucleophilic substitution. J. Nucl. Med. 27, 235-238.

Hahn T. and Desoye G. (1996). Ontogeny of glucose transport systems in the placenta and its progenitor tissues. Early Pregnancy 2, 168-182.

Hard G.C. (1985). Differential renal tumor response to N-ethylnitrosourea and dimethylnitrosamine in the Nb rat: basis for a new rodent model of nephroblastoma. Carcinogenesis 6, 1551-1558.

Hard G.C. and Butler W.H. (1970). Cellular analysis of renal neoplasia: induction of renal tumors in dietary conditioned rats by dimethylnitrosamine, with a reappraisal of morphological characteristics. Cancer Res. 30, 2796-2805.

Hard G.C. and Butler W.H. (1971a). Ultrastructural study of the development of interstitial lesions leading to mesenchymal neoplasia int he rat renal cortex by dimethylnitrosamine. Cancer Res. 31, 337-347.

Hard G.C. and Butler W.H. (1971b) Ultrastructural analysis of renal mesenchymal tumor induced in rat by dimethylnitrosamine. Cancer Res. 31, 348-365.

Hauguel-De Mouzon S., Challier J.C., Kacemi A., Caüzac M., Malek A. and Girard, J. (1997). The GLUT-3 glucose transporter isoform is differentially expressed within human placental cell types. J. Clin. Endocrinol. Metab. 82, 2689-2694.

IARC. International Agency for Research on Cancer. (1978). Some N-nitroso compounds. IARC monographs on the evaluation of carcinogenic risk of chemical to humans. Vol. 17, Lyon, France. p 365.

IARC. International Agency for Research on Cancer. (1982). Chemicals, industrial processes and industries associated with cancer in humans. IARC monographs on the evaluation of carcinogenic risk of chemicals to humans. Suppl. 4. Lyon, France. p 292.

Khandani A.H., Whitney K.D., Keller S.M., Isasi C.R. and Donald Blaufox M. (2007). Sensitivity of FDG PET, GLUT-1 expression and proliferative index in bronchioloalveolar lung cancer. Nucl. Med. Commun. 28, 173-177.

Langenskiöld M., Holmdahl L., Falk P., Angenete E. and Ivarsson M.L. (2008). Increased TGF-Beta1 protein expression in patients with advanced colorectal cancer. J. Surg. Oncol. 97, 409-415.

Larson S.M., Weiden P.L., Grunbaum Z., Kaplan H.G., Rasey J.S., Graham M.M., Sale G.E., Harp G.D. and Williams D.L. (1981). Positron imaging feasibility studies. II: Characteristics of 2-deoxyglucose uptake in rodent and canine neoplasms: concise communication. J. Nucl. Med. 22, 875-879.

Magee P.N. and Barnes J.M. (1962). Induction of kidney tumours in the rat with dimethylnitrosamine (N-nitroso-dimethylamine). J. Pathol. Bacteriol. 84, 19-31.

Maher F., Vanucci S., Takeda J. and Simpson I. (1992). Expression of mouse GLUT-3 and human GLUT-3 glucose transporter proteins in brain. Biochem. Biophys. Res. Commun. 182, 703-711.

Marian T., Balkay L., Krasznai Z. and Tron L. (2000). Membrane permeability changes induce hyperpolarization in transformed lymphoid cells under high density culture conditions. Cytometry 41, 186-192.

Meneses A.M., Medina R.A., Kato S., Pinto M., Jaque M.P., Lizama I., García Mde L., Nualart F. and Owen G.I. (2008). Regulation of GLUT-3 and glucose uptake by the camp signalling pathway in the breast cancer cell line ZR-75. J. Cell Physiol. 214, 110-116.

Mückler M. (1990). Family of glucose-transporter genes. Implications for glucose homeostasis and diabetes. Diabetes 39, 6-11.

Nishioka T., Oda Y., Seino Y., Yamamoto T., Inagaki N., Yano H., Imura H., Shigemoto R. and Kikuchi H. (1992). Distribution of the glucose transporters in human brain tumors. Cancer Res. 52, 3972-3979.

Paragh G., Kertai P., Kovacs P., Paragh G. Jr, Fülöp P. and Foris G. (2003). HMG CoA reductase inhibitor fluvastatin arrests the development of implanted hepatocarcinoma in rats. Anticancer Res. 23, 3949-3954.

Peto R., Gray R., Brantom P. and Grasso P. (1984). Nitrosamine carcinogenesis in 5120 rodents: Chronic administration of sixteen different concentrations of NDEA, NDMA, NPYR and NPIP in the water of 4440 inbread rats, with parallel studies on NDEA alone of the effect of age starting (3, 6 or 20 weeks) and of species (rats, mice, hamsters). IARC Sci. Publ., Lyon, France. 57, 627-665.

Rastogi S., Banerjee S., Chellappan S. and Simon G.R. (2007). GLUT-1 antibodies induce growth arrest and apoptosis in human cancer cell lines. Cancer Lett. 257, 244-251.

Rizzino A. (1993). Understanding the roles of growth factors in carcinogenesis modulation of autocrine growth control by differentation. Int. J. Dev. Biol. 37, 61-65.

Sittig M. (1985). Handbook of toxic and hazardous chemicals and carcinogens. 2nd ed. Noyes Publications. Park Ridge, N.J. pp 950.

Slagel D.E., Desimone P., Dillon M., Lepage D.J. and Bogden A.E. (1985). Subrenal capsule assay: feasibility of transporting tissues to a central facility for testing. Cancer Treat. Rep. 69, 717-718.

Som P., Atkins H.L., Bandoypadhyay D., Fowler J.S., MacGregor R.R., Matsui K., Oster Z.H., Sacker D.F., Shiue C.Y., Turner H., Wan C.N., Wolf A.P. and Zabinski S.V. (1980). A fluorinated glucose analog, 2-fluoro-2-deoxy-D-glucose (F-18): nontoxic tracer for rapid tumor detection. J. Nucl. Med. 21, 670-675.

Tomatis L. (1973). Transplacental carcinogenesis. In: Modern trends in oncology. Part I. Raven R.W. (ed). Butterworths. London.

Tsukioka M., Matsumoto Y., Noriyuki M., Yoshida C., Nobeyama H., Yoshida H., Yasui T., Sumi T., Honda K. and Ishiko O. (2007). Expression of glucose transporters in epithelial ovarian carcinoma: correlation with clinical characteristics and tumor angiogenesis. Oncol. Rep. 18, 361-367.

Trencsényi G., Kertai P., Somogyi C., Nagy G., Dombradi Z., Gacsi M. and Banfalvi G. (2007). Chemically induced carcinogenesis affecting chromatin structure in rat hepatocarcinoma cells. DNA Cell. Biol. 26, 649-655.

Trencsenyi G., Kertai P., Bako F., Hunyadi J.,Marian T., Hargitai Z., Pocsi I., Muranyi E., Hornyak L. and Banfalvi G. (2009). Renal capsule. Parathymic lymph node complex: A new in vivo metastatic model in rats. Anticancer Res. 29, 2121-2126.

Usatoff V. and Habib N.A. (2000). Hepatocellular carcinoma. The clinical problem. In: Hepatocellular carcinoma: Methods and protocols. Habib N.A. (ed). Humana Press Inc. Totowa. NJ pp 3-20.

Uzvolgyi E., Katona A. and Kertai P. (1990). Tumor cell implantation with the use of Gelaspon gelatin sponge disc. Cancer Lett. 51, 1-5.

Von Wolff M., Ursel S., Hahn U., Steldinger R. and Strowitzki T. (2003). Glucose Transporter Proteins (GLUT) in human endometrium: Expression, regulation, and function throughout the menstrual cycle and in early pregnancy. J. Clin. Endocrinol. Metab. 88, 3885-3892.

Wahl L.R. (1996). Targeting glucose transporters for tumor imaging: “sweet” idea, "sour" result. J. Nucl. Med. 37, 1038-1041.

Waki A., Kato H., Yano R., Sadato N., Yokoyama A., Ishii Y., Yonekura Y. and Fujibayashi Y. (1998). The importance of glucose transport activity as the rate-limiting step of 2-deoxyglucose uptake in tumor cells in vitro. Nucl. Med. Biol. 25, 593-597.

Yamamoto T., Seino Y., Fukumoto H., Koh G., Yano H., Inagaki N., Yamada Y., Inoue K., Manabe T. and Imura H. (1990). Over-expression of facilitative glucose transporter genes in human cancer. Biochem. Biophys. Res. Commun. 170, 223-230.

Younes M., Le chago L.V., Somoano J.R., Mosharaf M. and Lechago J. (1997). Immunohistochemical detection of glut 3 in human tumors and normal tissues. Anticancer Res. 17, 2747-2750.

Accepted September 25, 2009